Analysis of states in 13C populated in 9Be+4He resonant scattering

Freer, M.; Ashwood, N. I.; Curtis, N.; Di Pietro, A.; Figuera, P.; Fisichella, M.; Grassi, L.; Jelavić Malenica, Deša; Kokalova, Tz.; Koncul, Mladen; ...

Source / Izvornik: **Physical Review C - Nuclear Physics, 2011, 84**

Journal article, Published version
Rad u časopisu, Objavljena verzija rada (izdavačev PDF)

https://doi.org/10.1103/PhysRevC.84.034317

Permanent link / Trajna poveznica: https://urn.nsk.hr/urn:nbn:hr:217:522195

Analysis of states in ^{13}C populated in ^{9}Be + ^{4}He resonant scattering

M. Freer,[1] N. I. Ashwood,[1] N. Curtis,[1] A. Di Pietro,[2] P. Figuera,[2] M. Fisichella,[2] L. Grassi,[3] D. Jelavić Malenica,[3] Tz. Kokalova,[1] M. Koncul,[3] T. Mijatović,[3] M. Milin,[4] L. Prepolec,[3] V. Scuderi,[2] N. Skukan,[3] N. Soić,[3] S. Szilner,[3] V. Tokić,[3] D. Torresi,[2] and C. Wheldon[1]

[1]*School of Physics and Astronomy, University of Birmingham, Birmingham B15 2TT, United Kingdom*

[2]*INFN, Laboratori Nazionali del Sud, Via S. Sofia 44, Catania, Italy*

[3]*Ruder Bošković Institute, Bijenička 54, HR-10000 Zagreb, Croatia*

[4]*Department of Physics, Faculty of Science, University of Zagreb, Bijenička 32, HR-10000 Zagreb, Croatia*

(Received 17 July 2011; revised manuscript received 23 August 2011; published 20 September 2011)

Measurements of ^{9}Be + α resonant scattering have been performed using the thick-target approach with a ^{4}He gas volume and a large-area silicon strip detector. ^{9}Be beam energies in the range 12 to 21.4 MeV were used to measure the ^{13}C excitation energy spectrum between 13.2 and 16.2 MeV. An R-matrix analysis has been performed to characterize the spins and widths of ^{13}C resonances, some of which have been proposed to be associated with a $3\alpha + n$ molecular band.

DOI: 10.1103/PhysRevC.84.034317 PACS number(s): 27.20.+n, 21.10.−k, 24.30.−v

I. INTRODUCTION

The structure of light nuclei offers a range of complex phenomena including cluster-like structures. For example, it has long been believed that the Hoyle state in ^{12}C (E_x = 7.65 MeV, 0^+) has a 3α-cluster structure (e.g., see Ref. [1]). Recent analysis indicates that this state may even be associated with an α-particle, Bose, gas [2]. At least the fact that this state possesses a well-developed cluster structure appears to be established. An extension to the idea of cluster-like structures in $N = Z$, even-even, nuclei has been explored by von Oertzen and co-workers [3,4] (and references therein). In this case neutrons added to the α clusters behave as though they are covalently exchanged between the α-particle cores. There is good evidence for such molecular structures in the neutron-rich beryllium isotopes [6]. However, the extension to three-centered clusters, with valence neutrons, has yet to be put on such a firm footing. In ^{13}C a pair of rotational bands have been identified, which are candidates for a linear arrangement of the three alpha-particles in which the neutrons are covalently exchanged between the three centers [4].

A similar structure has also been found in the very recent cluster model calculations [5], where rather than a linear configuration a slightly bent structure is found. The linear structure would give rise to two bands of opposing parity with $K^{\pi} = 3/2^{\pm}$. Although many of the lower energy, and spin, members of the two bands are firmly assigned, significant uncertainty remains, particularly at higher energies. The proposed members of the bands are shown in Table I (see Ref. [4] for the associated energy-level diagram).

Here we use the ^{9}Be + α reaction to populate states in ^{13}C to probe the higher energy region associated with the proposed bands. This reaction is particularly appealing in terms of the population of molecular states in ^{13}C since in the ground state the ^{9}Be nucleus has a well-developed α-n-α molecular structure [6]. The intention is to test the proposed spin assignments of the ^{13}C molecular states using the current reaction.

II. EXPERIMENTAL DETAILS

The measurements were performed at the Ruder Bosković Institute tandem facility in Zagreb. Resonant scattering of the ^{9}Be beam was performed using a helium (^{4}He) gas volume in which a single large-area (5×5 cm^2) silicon detector was positioned at 0° to detect α particles emitted from the ^{4}He(^{9}Be, ^{4}He) reaction. The helium gas pressure was adjusted so as to stop the ^{9}Be beam $\sim$5 cm in front of the detector. The helium gas was contained within a reaction chamber using a 2 μm Havar foil. Beam energies of 12, 17, 20, and 21.4 MeV were used with helium gas pressures of 460, 820, 955, and 1020 mbar, respectively. Typical beam currents were $\leqslant$1 pnA. The silicon detector was a 1 mm thick double-sided silicon-strip detector. Each face was subdivided into 16 strips (vertical on the back and horizontal on the front) providing effectively 256 pixels. The silicon detector was placed 42 cm from the Havar window. Calibration of the detector was performed using elastic scattering of 12 and 16 MeV ^{7}Li nuclei from a ^{197}Au foil with the silicon detector placed at 44° with respect to the beam axis. The typical energy resolution of each strip was 100 keV. The experimental setup is shown in Fig. 1.

III. ANALYSIS AND RESULTS

Events in which a single front strip and a single rear strip recorded an energy in excess of 1 MeV were selected. Further, the energy difference between the front and back was restricted to be less than 250 keV. For such events the emission angles with respect to the beam axis, measured from the Havar window, were also calculated.

Assuming the detected particle to be an α particle the energy loss through the gas was calculated. This was performed by calculating the energy loss of the ^{9}Be beam at each point along the path through the gas volume using the energy-loss code DEDX [7]. This permitted the energy of the α particle emitted in the ^{4}He(^{9}Be, ^{4}He) reaction to be determined and hence the energy loss from the interaction point to the detector. These

TABLE I. Possible molecular bands in ^{13}C associated with $K^\pi = 3/2^\pm$ from [4].

J^π proposed	E_x (MeV)	J^π assignment in Ref. [13]	Γ from [13] (keV)
$K^\pi=3/2^-$			
$3/2^-$	9.897	$3/2^-$	26
$5/2^-$	10.818	$5/2^-$	24
$7/2^-$	12.438	$7/2^-$	336
$9/2^-$	14.13	$3/2^-$	150
$11/2^-$	16.08	$(7/2^+)$	150
$K^\pi = 3/2^+$			
$3/2^+$	11.080	$1/2^-$	$\leqslant$4
$5/2^+$	11.950	$5/2^+$	150
$7/2^+$	13.41	$(9/2^-)$	35
$9/2^+$	15.28	$9/2^+$	None
$11/2^+$	16.950	None	330

calculations were then fitted with a polynomial function such that for every detected α particle it was possible to calculate the energy upon emission in the reaction and hence the center-of-mass energy. The energy-loss calculations provided an accurate determination of the energies of known resonances in ^{13}C, whereas it is known that other energy-loss calculations are less accurate [8]. In the current analysis it was assumed that the influence of the beam on the gas properties was negligible given the significant heat capacity of the gas. The gas temperature was monitored and no significant variation was observed. The accuracy of the energy-loss calculation would confirm this conclusion.

In order to correct for the variation of the angular acceptance of the silicon detector as a function of the distance of interaction point with respect to the Havar window a series of Monte Carlo simulations were performed. These simulated the energy

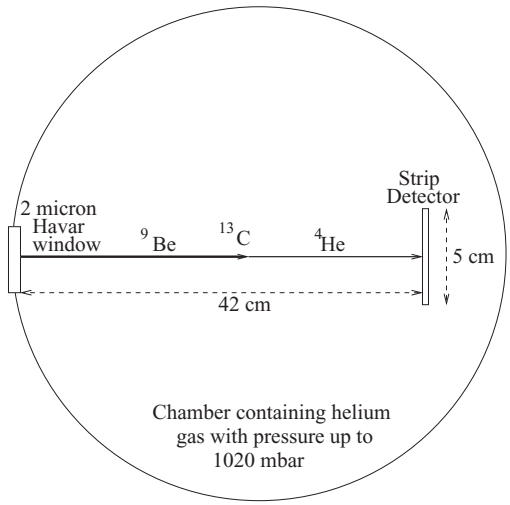

FIG. 1. Experimental setup showing the ^{9}Be beam passing through the Havar window, interacting with a ^{4}He nucleus to form ^{13}C, with the subsequent emission of an α particle in the forward direction. The α particle is then detected by the silicon strip detector. The gas pressure is then adjusted to stop the beam in the gas before the detector.

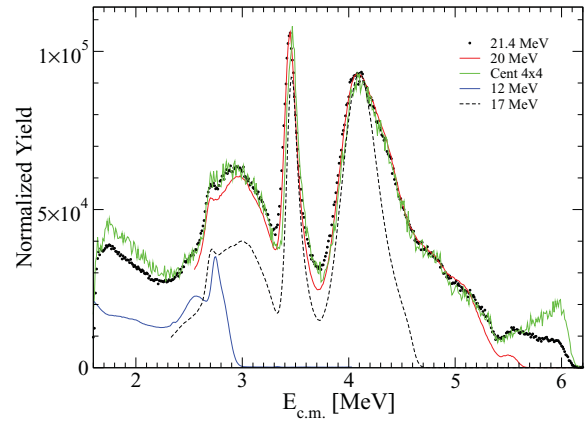

FIG. 2. (Color online) The excitation function for ^{9}Be + α measured at 21.4 MeV (black dots), 20 MeV (red line), 17 MeV (dashed line), and 12 MeV (blue line). The 21.4 MeV data restricted to the central 4×4 pixels are shown by the green line.

loss of the beam through the gas, the ^{9}Be + ^{4}He interaction assuming an isotropic center-of-mass angular distribution for the breakup, and the subsequent energy loss of the α particle through the gas volume. The emission angle of the α particle was then checked to determine whether it was within the angular acceptance of the silicon detector. The corresponding ^{9}Be + ^{4}He center-of-mass energy spectra were then divided by the calculated efficiency. The resulting center-of-mass energy spectra are shown for the various beam energies in Fig. 2.

These spectra reveal resonances which may be associated with ^{13}C excited states. The spectra at the various beam energies show a good degree of internal consistency. For example, the measurements at 20 and 21.4 MeV coincide almost perfectly. The spectrum corresponding to the 17 MeV beam energy also shows many of the features of the two higher energy measurements, but possesses a reduced strength at the lower center-of-mass energies. This spectrum is very similar to that determined in Ref. [8] up to $E_{\text{c.m.}} = 4.2$ MeV. The resonant scattering process may result in the formation of a resonance in ^{13}C which then decays to excited states in ^{9}Be, all of which are neutron unbound. In addition, due to the weak binding of the ^{9}Be nucleus it is possible that the projectile might break up into $2\alpha + n$, in which one, or more, of the α particles are detected. In the present measurements such processes are indistinguishable from the elastic resonant scattering. However, their contribution to the 20 and 21.4 MeV spectra may be estimated from the difference to the 17 MeV spectra. The 21.4 MeV spectrum is shown together with this estimated contribution from inelastic scattering processes (dotted line) in Fig. 3.

The measured spectrum presented in Fig. 3 corresponds to the detection of the α particles emitted in the forward direction in the laboratory frame, $\sim$180 $^\circ$ in the center-of-mass frame, but over the full angular range of the detector. However, due to the finite acceptance of the detector this includes a range of scattering angles away from 180 $^\circ$, particularly for events in which the reaction takes place close to the detector. In order to quantify the variation in the shape of the spectrum arising from the large angular acceptance, the spectrum is also shown

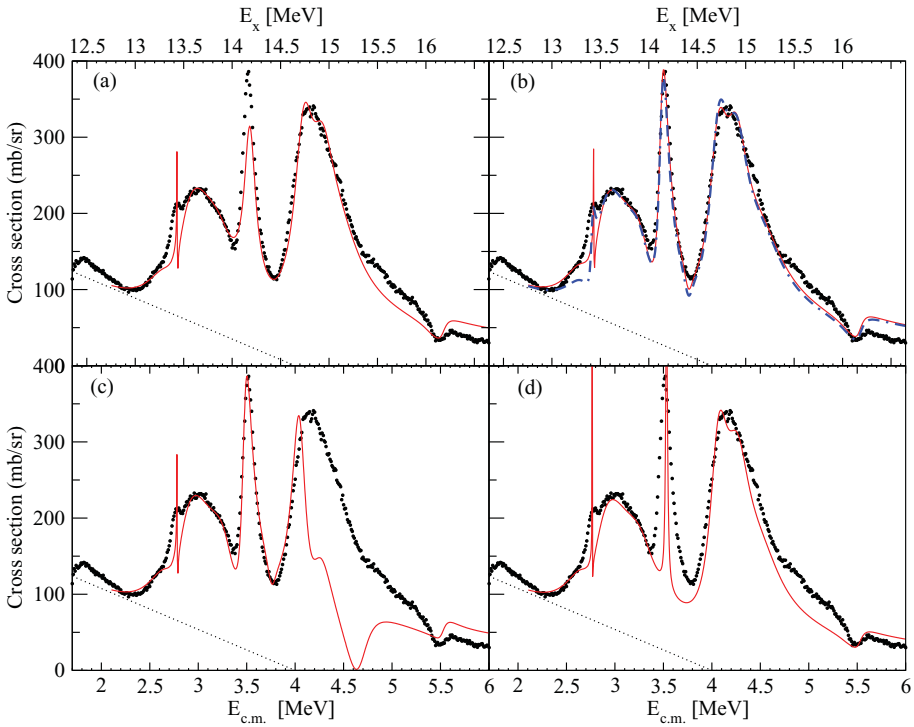

FIG. 3. (Color online) R-matrix fits [red lines and blue dot-dashed line in (b)] to the 21.4 MeV data (black points). The dotted line shows the estimated background contribution from breakup and inelastic contributions. See the main text for details. Parts (a) and (b) are labeled in terms of the ^{13}C excitation energy and (c) and (d) the center-of-mass energy of the $\alpha + {}^{9}$Be system. $E_x = E_{\text{c.m.}} + 10.65$ MeV.

in Fig. 2 corresponding to the center 16 pixels (4×4) of the detector. This corresponds to an area of 12.5×12.5 mm^2. The 21.4 MeV spectrum for the full detector and for the restricted area are identical except at the extremes of the spectrum. At higher energies the normalized yield is larger for the 4×4 spectrum. This is due to the presence of a collimating aperture mounted on the window which obscured the view of the larger angle elements of the detector of events occurring close to the window. The yield is also slightly larger at the lower energies.

The yield has been converted to cross section (mb/sr) in Fig. 3 by normalizing the data to the calculated Rutherford scattering cross section at the low-energy ($E_{\text{c.m.}} < 2$ MeV) part of the spectrum. This results in a cross section for the $E_{\text{c.m.}} = 3.5$ MeV peak of 360 mb/sr (after background subtraction). Previous measurements of the ^{9}Be(^{4}He, ^{4}He) reaction, in which rather than the thick target approach the beam energy was varied, found cross sections of 140, 220, and 320 mb/sr for this peak at $\theta_{\text{c.m.}} = 156^\circ$, 167.2°, and 171.6°, respectively [9,10]. The current measurements correspond to $\theta_{\text{c.m.}} \simeq 180^\circ$ and hence are consistent with the observed trend. Nevertheless, it is estimated there is an overall systematic error in the calculated cross section of ∼20%. This estimate is based on the degree to which the low-energy cross section can accurately be matched to the Rutherford scattering cross section at low energy. The center-of-mass, excitation, energy resolution is dominated by the energy resolution of the detector and hence is estimated to be (FWHM) 30 keV ($R = [4/(4+9)]100$ keV).

To characterize the resonances observed in the experimental spectrum, a series of R-matrix calculations have been performed [11,12]. These calculations simulate resonances in a nuclear potential with a radius given by $r = 1.3(9^{1/3} + 4^{1/3})$ fm (the α-particle channel radius). In the present approach, both the decay to the $^{9}\text{Be}_{\text{gs}} + \alpha$ and $^{12}\text{C}_{\text{gs}} + n$ channels are included. Hence it is possible to infer information regarding the partial decay widths Γ_α and Γ_n. The magnitude of peaks in the resulting excitation energy spectrum is proportional to $(2J+1)\Gamma_\alpha^2$ (J being the resonance spin) and the width is given by $\Gamma = \Gamma_\alpha + \Gamma_n$. In this manner it is possible to gain an insight into the spin and partial widths of the experimentally observed resonances. In turn, the partial widths are related to the reduced widths, γ_α via $\Gamma_\alpha = 2P_L\gamma_\alpha^2$ (for α decay), where P_L is the R-matrix penetrability (i.e., the barrier penetrability multiplied by kr, k being the wave number describing the center-of-mass motion and r the channel radius described above) for a given orbital angular momentum L. The widths of the states are thus also sensitive to the spin of the resonance via the orbital angular momentum required for the formation and the effect of the centrifugal barrier.

The parameters used in these calculations are summarized in Table II. The proposed assignments for the $K^\pi = 3/2^\pm$ molecular bands from Ref. [4] were shown in Table I. The following presents an analysis of the experimental data in light of the proposed molecular assignments and previous tabulations of excited states in ^{13}C.

Figure 3 presents a series of such R-matrix calculations which have been fitted to the experimental data after the background subtraction indicated by the dotted lines. Parts (a) and (b) of the figure show the fits to the data using parameters which are close to those found in Tables 13.4 and 13.8 in Ref. [13]. Table 13.4 represents the accepted values of states in ^{13}C as compiled by Ajzenberg-Selove, while Table 13.8 corresponds to resonance parameters previously determined from an analysis of the ^{9}Be(α,α_0) reaction [9]. From the present measurements it is possible to estimate that the decay contribution to the ^{9}Be excited states is relatively minor. As noted above, the neutron

TABLE II. Parameters used in the R-matrix fit shown in Fig. 3, compared with those from the compilation of ^{9}Be(α, α_0) resonances presented in Table 13.4 of Ref. [13].

Ref. [13] Table 13.4				Fig. 3(a)					Fig. 3(b)				
E_x (MeV)	$E_{\text{c.m.}}$ (MeV)	J^π	Γ	$E_{\text{c.m.}}$ (MeV)	J^π	Γ	Γ_α	Γ_n	$E_{\text{c.m.}}$ (MeV)	J^π	Γ	Γ_α	Γ_n
13.28	2.63	$(3/2^-)$	340	2.73	$3/2^-$	340	294	46	2.73	$3/2^-$	340	294	46
13.41	2.76	$(9/2^-)$	35	2.78	$9/2^-$	2	2	0	2.78	$9/2^-$	2	2	0
13.57	2.92	$7/2^-$	620	2.88	$7/2^-$	628	557	71	2.88	$7/2^-$	596	512	84
13.76	3.11	$(5/2, 3/2)^+$	300	3.24	$5/2^+$	335	39	296	3.28	$5/2^+$	337	103	234
14.13	3.48	$3/2^-$	150	3.55	$3/2^-$	179	179	0	3.48	$5/2^-$	124	124	0
14.39	3.74	$(1/2, 5/2)^-$	280	3.81	$7/2^-$	293	24	269	3.76	$7/2^-$	111	12	99
14.58	3.93	$(7/2, 9/2)^+$	230	4.09	$9/2^+$	271	218	53	4.07	$9/2^+$	285	244	41
14.983	4.333	$(7/2^-)$	380	4.33	$7/2^-$	418	250	168	4.31	$7/2^-$	406	238	168
15.27	4.62	$9/2^+$		4.50	$5/2^-$	493	154	339	4.50	$5/2^-$	493	154	339
15.526	4.876	$(3/2^-)$	150										
16.08	5.43	$(7/2^+)$	150	5.51	$7/2^+$	140	21	119	5.51	$7/2^+$	140	21	119
16.15	5.5	$(5/2^-)$	230	5.49	$5/2^-$	253	23	230	5.49	$5/2^-$	253	23	230

decay channel, which has a threshold 5.7 MeV lower than the α-decay threshold (the α-decay threshold is 10.65 MeV), is introduced in order to reproduce the experimental cross sections and the previously reported widths. Figure 3 part (a) shows the fit corresponding to the adopted ^{13}C level parameters (Ref. [13], Table 13.4) and the red line in part (b) shows the analysis using resonance parameters taken from the tabulations of the ^{9}Be(α, α_0) reaction (Ref. [13], Table 13.8).

The essential difference between the two fits concerns the spin and parities for resonances between 14.0 and 14.5 MeV ($E_{\text{c.m.}} = 3.35$ to 3.85 MeV). In the adopted levels there are resonances at 14.13 and 14.39 MeV with $J^\pi = 3/2^-$ and $(1/2, 5/2)^-$, respectively. In the ^{9}Be(α, α_0) reaction resonances are found at 14.11 and 14.16 MeV with $J^\pi = 5/2^-$ and $7/2^+$ (or $7/2^-$), respectively. The 14.11 MeV state is almost certainly the 14.13 MeV state listed in Table 13.4 in Ref. [13]. In the present analysis it was found that for a better reproduction of the minima close to the $E_{\text{c.m.}} = 3.5$ MeV peak that the state at 14.16 MeV should be $7/2^-$. It is clear that with this single modification the current data are more closely reproduced with the previously recorded ^{9}Be(α, α_0) resonances with widths very close to those found earlier. However, with the inclusion of the $J^\pi = 3/2^-$ at $E_{\text{c.m.}} \simeq 3.5$ MeV ($E_x = 14.15$ MeV) it is not possible to reproduce the strength and width of the prominent resonance at this energy [Fig. 3(a)]. This latter figure illustrates the case where $\Gamma_\alpha = \Gamma$. Hence, it is not possible to increase the amplitude of the resonance without simultaneously also increasing the width beyond that which is observed experimentally. Similarly, in Fig. 3(d) we examine the possibility that the state observed at $E_x = 14.13$ MeV, $E_{\text{c.m.}} = 3.48$ MeV, could possibly be identified with $J^\pi = 9/2^-$ as suggested in Ref. [4] (see our Table I). The current analysis indicates that it is not possible to reproduce simultaneously both the cross section and observed width with such an assignment. Due to the presence of a significant centrifugal barrier ($L = 4$) the α penetrability is relatively small. Thus, we conclude that the resonance tabulated at 14.13 MeV ($E_{\text{c.m.}} = 3.48$ MeV) should be associated with $J^\pi = 5/2^-$ and not $J^\pi = 3/2^-$ or $J^\pi = 9/2^-$.

The tabulations for ^{13}C [13] (Table 13.4) indicate the existence of a tentative $9/2^-$ at $E_x = 13.41$ MeV ($\Gamma = 35 \pm 3$ keV), which can also be found in the tabulated resonances observed in the ^{9}Be(α, α_0) measurements: 13.42 MeV, $(9/2^-)$, $\Gamma = 58$ keV. It can be observed from Fig. 3 and Table II that it is very difficult to generate a $9/2^-$ state at this energy with a width close to the above two values, due to the considerable centrifugal barrier, $L = 4$. It is suggested in Ref. [4] that this should rather be a $7/2^+$ state. The blue dot-dashed line in Fig. 3(b) indicates an R-matrix analysis using parameters similar to those used to calculate the red, solid, line in the same figure but with a $7/2^+$ state rather than $9/2^-$. The calculation is able to produce a state with a width of 60 keV which reproduces the experimental data, aside from the interference on the lower energy side of the resonance. However, the lowest beam energy data shown in Fig. 2 do indicate a possible interference which is perhaps obscured at the higher energies. Hence, it would appear probable that the state is not associated with $9/2^-$ character and could be $7/2^+$.

Figure 3(c) indicates the effect of the introduction of a $9/2^+$ resonance close to $E_x = 15.27$ MeV as suggested in Ref. [4]. This interferes strongly with either the $7/2^+$ or $9/2^+$ state at 14.58 MeV (here assumed to be $9/2^+$, though the conclusions would remain the same if $7/2^+$ were selected). It can be concluded that it is not possible to have two $9/2^+$ states (or a $9/2^+$ and a $7/2^+$ state) in such close proximity and that either the assignment of the 14.58 MeV or 15.27 MeV state is incorrect or that the 15.27 MeV state has a vanishingly small alpha-decay width. In the present analysis the choice of a $5/2^-$ state close to this latter energy ($E_x = 15.15$ MeV) appears to give the best reproduction of the experimental data.

IV. SUMMARY AND CONCLUSIONS

Measurements of the ^{9}Be + α resonant scattering over the energy range $E_x(^{13}\text{C}) = 13.2$ to 16.2 MeV ($E_{\text{c.m.}} = 2.6$ to 5.5 MeV), where the α particle is detected at $\theta_{\text{lab}} = 0^\circ$, $\theta_{\text{c.m.}} = 180^\circ$, have been analyzed using the multichannel

R-matrix framework. Both α-decay and neutron-decay channels were included for decays to the ^{9}Be and ^{12}C ground states. The current analysis is broadly consistent with the single-level analysis reported in Table 13.8 [13] (taken from Ref. [9]). This would confirm that the 14.13 MeV state should have an assignment of $5/2^-$ (as opposed to the adopted $3/2^-$) and that it is unlikely that the resonance has $J^\pi = 9/2^-$ as suggested in Ref. [4]. Similarly, it is unlikely that there is a strong contribution to the data from a $9/2^+$ resonance at 15.27 MeV, which may indicate an alternative spin or a very small α-decay width. These conclusions may require some adjustment to states assigned to the proposed molecular bands in ^{13}C in Ref. [4]. However, the proposed existence of a $7/2^+$ state at 13.41 MeV associated with a molecular band is supported by the current analysis. There are several possibilities as to the nature of the high-spin ($\geqslant 9/2$) members of the molecular band. It is possible that the band becomes unstable beyond $J = 7/2$, or that the states are weakly populated in the present measurements. The current analysis would indicate, for example, that the $9/2^-$ state should have a rather narrow width. It is possible that it is thus unresolved from the dominant $5/2^-$ state at 15.27 MeV. Measurements over a wider angular range than covered here might be able to further resolve this question.

ACKNOWLEDGMENTS

TzK acknowledges the financial support of the Daphne Jackson Trust.

[1] D. M. Brink, in *Proc. Int. School of Physics Enrico Fermi, Course XXXVI, Varenna, 1966*, ed. C. Bloch (Academic Press, New York, 1966).
[2] A. Tohsaki, H. Horiuchi, P. Schuck, G. Röpke Phys. Rev. Lett. **87**, 192501 (2001).
[3] W. von Oertzen *et al*., Eur. Phys. J. A **21**, 193 (2004).
[4] M. Milin and W. von Oertzen, Eur. Phys. J. A **14**, 295 (2002).
[5] N. Furutachi and M. Kimura, Phys. Rev. C **83**, 021303(R) (2011).
[6] W. von Oertzen, M. Freer, and Y. Kanada En'yo, Phys. Rep. **432**, 43 (2006).
[7] Energy-loss code DEDX (unpublished).
[8] M. Zadro *et al*., Nucl. Instrum. Methods Phys. Res. Sect. B **259**, 836 (2007).
[9] J. D. Gross, S. L. Blatt, D. R. Parsignault, C. D. Porterfield, and F. L. Rifle, Phys. Rev. C **7**, 1837 (1973).
[10] J. Liu, Z. Zheng, and W. K. Chu, Nucl. Instrum. Methods B **108**, 247 (1996).
[11] A. M. Lane and R. G. Thomas, Rev. Mod. Phys. **30**, 257 (1958).
[12] R-matrix code courtesy of G. Rogachev.
[13] F. Ajzenberg-Selove, Nucl. Phys. A **523**, 1 (1991).